

The Star Formation History of intermediate redshift late-type galaxies

Ignacio Ferreras^{1,2?}, Joseph Silk¹, Asmus Böhm³, Bodo Ziegler³

¹*Physics Dept. Denys Wilkinson Building, Keble Road, Oxford OX1 3RH*

²*Institut für Astronomie, Swiss Federal Institute of Technology (ETH), Hönggerberg Campus, HPF D8, CH-8093 Zürich, Switzerland*

³*Universitätssternwarte Göttingen, Geismarlandstrasse 11, D-37083 Göttingen, Germany*

Accepted for publication in MNRAS, August 9, 2004

ABSTRACT

We combine the latest observations of disk galaxy photometry and rotation curves at moderate redshift from the FORS Deep Field (FDF) with simple models of chemical enrichment. Our method describes the buildup of the stellar component through infall of gas and allows for gas and metal outflows. In this framework, we keep a minimum number of constraints and we search a large volume of parameter space, looking for the models which best reproduce the photometric observations in the observed redshift range ($0.5 < z < 1$). We find the star formation efficiency to correlate well with v_{MAX} so that massive disks are more efficient in the formation of stars and have a smaller spread in stellar ages. This trend presents a break at around $v_{\text{MAX}} \approx 140 \text{ km s}^{-1}$. Galaxies on either side of this threshold have significantly different age distributions. This break has been already suggested by several authors in connection with the contribution from either gravitational instabilities or supernova-driven turbulence to star formation. The gas infall timescale and gas outflows also present a correlation with galaxy mass, so that massive disks have shorter infall timescales and smaller outflow fractions. The model presented in this paper suggests massive disks have formation histories resembling those of early-type galaxies, with highly efficient and short-lived bursts, in contrast with low-mass disks, which have a more extended star formation history. The ages correlate well with galaxy mass or luminosity, and the predicted gas-phase metallicities are consistent with the observations of local and moderate redshift galaxies. One option to explain the observed shallow slope of the Tully-Fisher relation at intermediate redshift could be small episodes of star formation in low-mass disks.

Key words: galaxies: spiral – galaxies: evolution – galaxies: formation – galaxies: stellar content.

1 INTRODUCTION

Quantifying the star formation history of galaxies constitutes one of the major unsolved issues towards a complete understanding of galaxy formation. Within the current paradigm of structure formation, disk galaxies represent the building blocks from which the whole zoo of galaxies is formed. A detailed analysis of galaxy formation histories is hindered by the complexity of star formation. By coupling simple assumptions about star formation and chemical enrichment to population synthesis models which track the evolution of well-defined stellar populations, one can constrain the possible scenarios of star formation in a semi-quantitative way. Furthermore, by exploring galaxies at high redshift one takes advantage of the lookback times which allow us to probe back into the past histories of these galaxies.

Disk galaxies have been complicated to analyze, mostly be-

cause of their ongoing star formation, dust and complex geometry which prevent us from getting a clear picture of their underlying stellar populations. Qualitatively, the photo-spectroscopic properties of disk galaxies such as our own Milky Way are compatible with a weak and continuous star formation rate (SFR) along with a stronger early episode of star formation whose amplitude correlates well with galaxy type, being stronger in disks of earlier types (e.g. Kennicutt 1998a).

Studies of disks at moderate and high redshift seem to yield a similar formation scenario. Lilly et al. (1998) observed a sample of 341 galaxies selected from the CFRS and the LDSS redshift surveys, out to $z < 1$, finding bluer $U - V$ colours and stronger [OII] emission at moderate redshift, which suggests an increase in the SFR by a factor of about 3 from local galaxies out to $z \approx 0.7$. However, the size function was not found to change with redshift, and the larger changes are associated with the smaller galaxies (however, see Giallongo et al. 2000; Vogt 2000). This is indicative of earlier formation of massive disks, in agreement with the

? E-mail: ferreras@phys.ethz.ch

lower gas fractions found in these systems (e.g. Bell & de Jong 2000). Boissier & Prantzos (2001) presented a detailed model of chemical enrichment in disk galaxies calibrated to the Milky Way (Boissier & Prantzos 1999). The application of this model to disk galaxies at moderate redshift showed that large disks have already completed their evolution by $z \approx 1$, whereas low-mass disks undergo a later evolution, resulting in a steepening of the slope of the Tully-Fisher relation with redshift. A similar conclusion is reached by Ferreras & Silk (2001) when comparing sets of simple chemical enrichment models over a wide range of parameter space using the $z = 0$ optical and NIR colour- v_{MAX} relation as a constraint. The star formation efficiency was found to correlate with galaxy mass, a point which is questioned by Boissier et al. (2001). However, this controversy hinges on the degeneracy between star formation efficiency and infall timescale. Both groups agree on the need for a rapid buildup of the stellar component in massive disks, a property that can be achieved either by a high efficiency of star formation or by a shorter infall timescale.

The evolution of the Tully-Fisher relation with redshift is a powerful discriminator of star formation histories. Vogt (2000) presented a sample of 100 faint disk galaxies in the range $0.2 < z < 1$ and no change was found in either shape or slope with respect to local samples. A zero point offset $< 0.2 - 0.3$ mag was found in the rest frame B band. Milvang-Jensen et al. (2003) explored cluster/field differences in the TF relation at moderate redshift on a smaller sample of 8 disk galaxies in cluster MS1054-03 ($z = 0.83$) as well as 19 field spirals in the $z = 0.15 - 0.9$ range. At fixed rotation velocity, they found cluster spirals to be $0.5 - 1$ mag brighter. However, their sample is too small to draw a firm conclusion on the evolution of the Tully-Fisher relation. In a larger sample of disk galaxies in 3 clusters at moderate redshift ($z \approx 0.5$) Ziegler et al. (2003) did not find significant differences with respect to field disks.

The work on 113 disk galaxies in the range $0.1 < z < 1.0$ from the FORS Deep Field on which this work is based (Böhm et al. 2004) revealed a striking result, namely a shallow slope of the rest frame B band Tully-Fisher relation with respect to local disks. Slowly rotating disks ($v_{\text{MAX}} < 100 \text{ km s}^{-1}$) at moderate redshift appear up to 2 magnitudes brighter than their low-redshift counterparts. One should question whether the samples at low and moderate redshift correspond to a simple one-to-one mapping. Indeed, the sample of Lilly et al. (1998) presents a large fraction of bright and small disks at $z \approx 1$ which do not have local counterparts.

In this paper, we combine photometric data from the FDF disk sample with a model which convolves galactic chemical evolution histories with stellar population synthesis in order to relate the photometric observations with a small set of phenomenological parameters which describe the major drivers of star formation in galaxies. We describe the observations in §2 and our model in §3. The results are discussed in §4 and the resulting ages and metallicities are presented in §5. Finally, in §6 we discuss our results and give the conclusions. Throughout this paper we use a Λ CDM cosmology with $\Omega_m = 0.3$ and $H_0 = 70 \text{ km s}^{-1} \text{ Mpc}^{-1}$, as suggested by the analysis of the angular power spectrum of the Cosmic Microwave Background observed by WMAP (Spergel et al. 2003). For this cosmology, the age of the Universe at $z = 0$ and $z = 1$ corresponds to 13.5 and 5.8 Gyr, respectively.

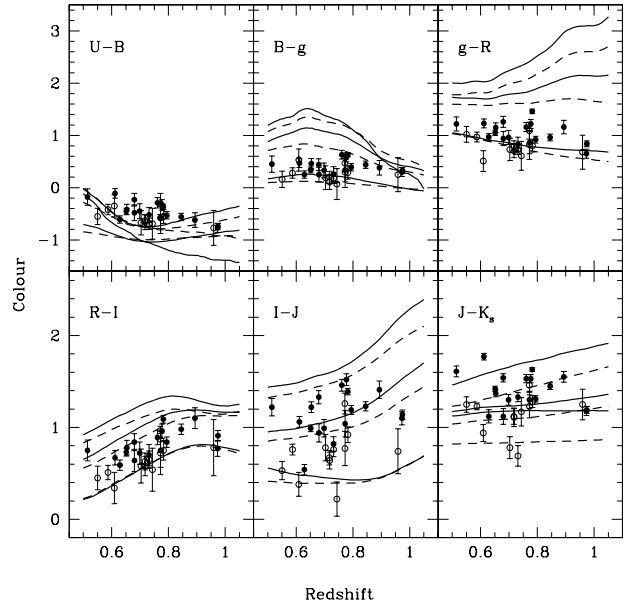


Figure 1. Colour-redshift plots of the sample of FDF moderate redshift disk galaxies used in this paper. The filled and empty dots represent galaxies with $\log v_{\text{MAX}} > 2.2$ and $6.2 \leq \log v_{\text{MAX}} < 6.5$, respectively. The lines correspond to the colours of simple stellar populations from the latest models of Bruzual & Charlot (2003), for three ages (from top to bottom): 8, 1, and 0.1 Gyr. For each age two metallicities are considered: Z_{\odot} (solid) and $Z = 3$ (dashed). Notice the bluer colours – which are most sensitive to young stars – suggest young stellar ages, whereas the red/NIR colours imply older ages.

2 OBSERVATIONS

We use a subsample of the data set presented by Ziegler et al. (2002) and Böhm et al. (2004) to study the redshift evolution of the Tully-Fisher relation. The galaxies are extracted from the FORS Deep Field (FDF), a deep (UBgRIJKs) survey over a $6^{\circ} \times 6^{\circ}$ area (Appenzeller et al. 2000). Spectroscopy with a resolution $R \approx 1200$ was carried out at FORS1 + 2 mounted on the VLT. Throughout this paper we refer to the intrinsic rotation velocities as v_{MAX} since these have been obtained from the flat part of the rotation curves. From the complete sample of 77 galaxies with measured v_{MAX} , we selected those at redshifts $z > 0.5$ resulting in a sample of 30 moderate redshift late-type galaxies, which cover a range of rotation velocity between 85 and 400 km s^{-1} . Figure 1 shows the colour-redshift diagrams of the $z > 0.5$ sample of FDF galaxies used in this paper. The photometry is performed over a 2 arcsec aperture, which corresponds to a projected physical size of $12 - 16 \text{ kpc}$ in the $z = 0.5 - 1$ redshift range. The magnitudes were corrected for galactic extinction, following Heidt et al. (2003) and intrinsic rest-frame extinction following Tully & Fouqué (1985), with the convention of a non-negligible extinction for face-on disks, so that the minimum value, e.g., in rest-frame B-band is $A_B = 0.27 \text{ mag}$. For more details on the sample reduction and v_{MAX} determination see Böhm et al. (2004). In the appendix we have explored the effect that a different dust correction would have on the model predictions. The lines in figure 1 show the colours for a set of simple stellar populations from the latest Bruzual & Charlot (2003) models for two metallicities: solar (solid lines) and $Z = 3$ (dashed lines), assuming three different ages (from top to bottom): 8, 1, and 0.1 Gyr. These are predictions

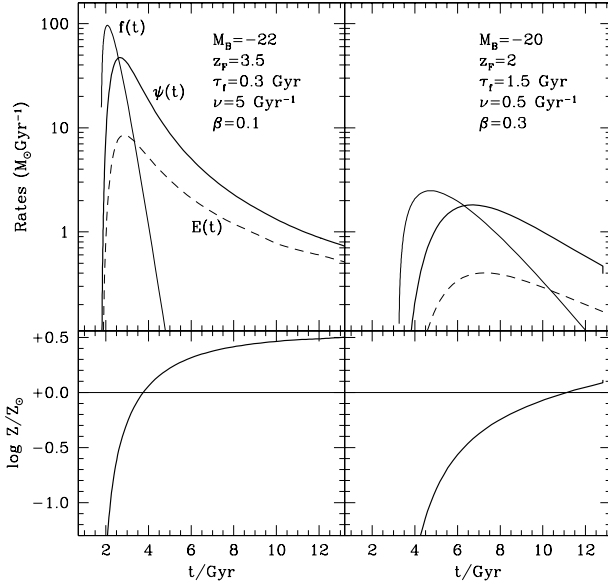


Figure 2. A sample of the generic star formation histories used in the modelling throughout this paper. The SFHs shown here give good fits to the colours of a massive ($M_B = -22$; left panel) and a lower-mass disk ($M_B = -20$; right panel). The top panels show the star formation rate ($f(t)$), which is driven by a Schmidt-type law fuelled by the infall of primordial gas ($\psi(t)$). The dashed line ($E(t)$) shows the contribution to the gas component from stars as they reach their endpoints of stellar evolution. The lower panels give the evolution of the metallicity with age. The parameters which correspond to each SFH are labelled in the top panels (see text for details). The mass rates are normalized to a final stellar mass content of 10^{11} (left) and $10^{10} M_\odot$ (right).

for simple populations with a single age and metallicity. Notice that the bluer colours – which are very sensitive to young stars – suggest young ages, whereas redder colours are more compatible with older ages. A more realistic composite model will take into account the different contributions from various ages and metallicities to each passband.

3 MODELLING THE SFH OF DISK GALAXIES

We consider a phenomenological scenario of star formation and chemical enrichment based on the models presented in Ferreras & Silk (2001). The rationale of our approach is to try to minimize the number of parameters describing the buildup of the stellar component. This enables us to run a fairly big number of realizations of these models, scanning a large volume of parameter space. We reduce the description of the process of star formation in galaxies to a few parameters, namely:

Star Formation Efficiency: Star formation is assumed to follow a variant of the Schmidt law (Schmidt 1959):

$$\dot{\rho}_*(t) = \frac{\rho_g(t)}{\rho_{TOT}}^n; \quad (1)$$

where ρ_g is the gas volume density and n is a parameter describing the star formation efficiency, which is an inverse timescale for the processing of gas into stars. ρ_{TOT} is the total baryon density,

which – for a single zone model – is just a fixed number throughout the analysis. The only purpose of including it in equation 1 is to give the units of an inverse timescale. Based on the best fit to observations from a local sample of normal spiral galaxies (Kennicutt 1998b) we decided to use $n = 1.5$. This exponent is also what one obtains for a star formation law that varies linearly with gas density and inversely with the local dynamical time: $\rho_g = \tau_{dyn}^{-1} \rho_g$.

Infall: The infall of primordial gas is described by a set of two parameters. We assume the infall rate – $\psi(t)$ – to be a delayed exponential function with an infall timescale (τ_F). We characterize the starting point at some epoch by a formation redshift z_F , so that the age of the Universe when the infall begins is $t(z_F)$. Defining $t = t - t(z_F)$, we can write the infall rate as:

$$\psi(t) = \frac{\rho_{TOT}}{\tau_F} e^{-t/\tau_F} \quad (2)$$

This function rises quickly to its maximum value at $t = \tau_F$ and then declines on a slower timescale. After a time $t_{90} = 3.9 \tau_F$ 90% of the total baryon content (ρ_{TOT}) has fallen on the galaxy. Notice that this choice of infall rate allows for a very wide of scenarios. Besides the standard model of a quickly rising rate with a slowly decaying branch, our parameter space also includes scenarios with an increasing infall rate – i.e. when long timescales ($\tau_F \sim 4-5$ Gyr) and late formation epochs ($z_F = 2$) are chosen. It is only the data that eventually constrain these scenarios.

Outflow fraction: The ejection of gas and metals from winds triggered by supernova explosions constitutes another important factor contributing to the final metallicity of the galaxy. We define a parameter ($0 \leq \beta \leq 1$) which represents the fraction of gas and metals from stellar ejecta and lost by the galaxy. Even though one could estimate a – model-dependent – value of β given the star formation rate and the potential well given by the total mass of the galaxy (e.g. Larson 1974, Arimoto & Yoshii 1987), we leave β as a free parameter, only to be constrained *a posteriori* by the data.

The stellar yields are simplified in the model by a truncated power law fitting the results from Van den Hoek & Groenewegen (2002) for Intermediate Mass Stars (IMS) (i.e. $M < 8 M_\odot$). The yields from massive stars – which undergo core-collapse – are obtained from Thielemann, Nomoto & Hashimoto (1996) assuming solar metallicity progenitors. A Salpeter (1955) IMF was used in the $0.1-60 M_\odot$ mass range. Other IMFs such as Chabrier (2003) were tested, to find no significant difference. After all, the slope of the IMF in the upper mass region – which mostly controls the chemical enrichment – is similar, and the colours do not vary significantly. The most important difference between these two IMFs is a systematic change in the stellar mass-to-light ratios. We refer the reader to Ferreras & Silk (2001) for details of the model applied to disk galaxies.

Figure 2 shows two sample star formation histories obtained by this parametrization. It corresponds to the best fits obtained for a typical massive (left) and low-mass disk (right). The parameters used for each one are given in the top panels. The star formation rate ($\dot{\rho}_*$), infall rate (ψ) and stellar ejecta (E) are shown, normalized to a final stellar mass content at $z = 0$ of 10^{11} (left) and $10^{10} M_\odot$ (right). The bottom panels give the evolution of the gas phase metallicity. Several models were run with formation redshifts between 2 and 5 and the results vary smoothly between these two extrema, which correspond to a formation time of 3.2 and 1.2 Gyr, respectively. More realistic models should have a well defined correlation between this formation redshift and the mass of the galaxy. However, in our spirit of keeping the number of constraints to a

minimum, we ran six grids of models for each galaxy with various values of z_F and chose the one with the minimum χ^2 . We want to emphasize that the trends presented in this paper are fairly robust and insensitive to the particular choice of z_F . The remaining three parameters (ϵ ; τ ; f) are explored over a large volume of parameter space as described in more detail below.

3.1 Data constraints

For each choice of parameters (ϵ ; τ ; f) we solve the chemical enrichment equations which give us a star formation history that is subsequently convolved with the latest population synthesis models of Bruzual & Charlot (2003) in order to generate a spectral energy distribution (sed) at the observed redshift of the galaxy under scrutiny ($0.5 < z < 1$). A χ^2 function is constructed by comparing the model prediction with the 2 arcsec aperture photometry. We define the χ^2 function as:

$$\chi^2 = \sum_{i=1}^6 \frac{[C_z(i) - C_z^m(i)]^2}{\sigma_z(i)^2}; \quad (3)$$

where $C_z(i)$ is the observed colour within a 2 arcsec aperture – which represents a physical projected distance between 12 and 16 kpc in the redshift range $0.5 < z < 1$. The fluxes were obtained from the coadded FDF images after convolving them to the same seeing – see Heidt et al. (2003) for details. The indices $i = f1; 2; 3; 4; 5; 6; g$ correspond to colours U, B, B_g, g, R, R_I, I, J and J_{Ks}, respectively. The photometric uncertainties in the colours are $\sigma_z(i)$ and are typically in the range $0.05 - 0.2$ mag. The model prediction in each filter is given by $C_z^m(i)$. For each model realization we compute the rest-frame B-band absolute luminosity at the redshift of the galaxy. These luminosities are normalized with respect to the observed apparent brightness in a passband closest to the rest-frame B band. In our sample this corresponds to R for $z < 0.85$ and I for $z > 0.85$ (Böhm et al. 2004). The total apparent magnitudes correspond to the MAG_AUTO algorithm of the Source Extractor package (Bertin & Arnouts 1996).

3.2 Finding the best fit

Searching for the choice of parameters which give the best fit according to the χ^2 function defined in the previous section is a rather computer-intensive endeavour. We decided to explore a set of 6 formation redshifts, namely $z_F = f2; 2.5; 3; 3.5; 4; 5; g$. The remaining three parameters, namely (ϵ ; τ ; f) are searched for each galaxy in our sample in a $32 \times 32 \times 32$ grid over a wide range of values, namely:

$$\begin{aligned} 1.3 &\leq \log(\epsilon = G \text{ yr}^{-1}) \leq 6 + 1.5, \\ 0.6 &\leq \log(\tau) \leq 6, \\ 1.3 &\leq \log(f = G \text{ yr}) \leq 6 + 0.7. \end{aligned}$$

The best fit to the data is determined by the maximization of the likelihood function $L(z_F; \epsilon; \tau; f) / \exp[-\frac{1}{2} \chi^2(z_F; \epsilon; \tau; f)]$, where $\chi^2(z_F; \epsilon; \tau; f)$ is described above. With the uncertainties inherent to any modelling of galactic chemical enrichment and given that the constraints used in this paper are only based on a few photometric measurements, we caution the reader to take these results as semi-quantitative trends. The strongest value of the model predictions lie in the *relative* difference between parameters among galaxies. In the following figures we show the best fits for each

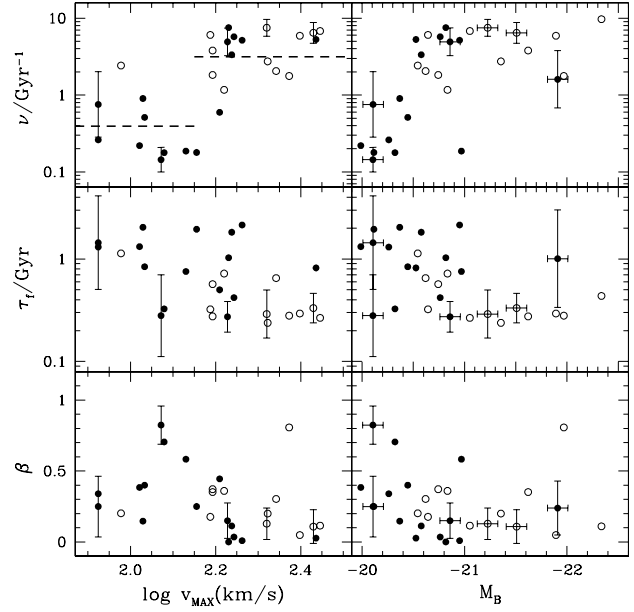


Figure 3. Predicted model parameters as a function of rotation velocity (*left*) or absolute B-band luminosity (*right*) for the complete ($z > 0.5$) FDF moderate redshift sample. The filled and hollow circles represent the $z < 0.75$ and $z > 0.75$ subsamples, respectively. Typical marginalized 1σ error bars are shown. The parameters are (from top to bottom) star formation efficiency (ϵ), infall timescale (τ), and outflow fraction (f). The dashed lines in the top panels represent the median value of the star formation efficiency, separating the sample at $v_{MAX} = 140 \text{ km s}^{-1}$.

galaxy along with the 1σ confidence level obtained by the likelihood function.

4 THE STAR FORMATION HISTORY OF DISK GALAXIES

Figure 3 shows the prediction for the best fit values of the parameters controlling the star formation history as a function of rotation velocity (*left*) or B-band luminosity (*right*). The sample is separated into a lower redshift ($0.5 \leq z < 0.75$; filled circles) and a higher redshift sub-sample ($z > 0.75$; hollow circles). Some typical (1σ) marginalised error bars are shown. Even though the uncertainties are rather large – as expected from any analysis based on broadband photometry – one can still hint at a significant correlation between the star formation efficiency (ϵ ; top panels) and rotation velocity. The dashed lines give the median of separating the sample at $v_{MAX} = 140 \text{ km s}^{-1}$. A clear increase in the star formation efficiency is seen for the more massive disks. Furthermore, the position of this “break” is reminiscent of the recent results of Kauffmann et al. (2003) on a large sample of 10^5 galaxies from the SDSS. Their study showed a clear bimodality in the distribution of age-sensitive observables such as the 4000Å break strength or H_δ Balmer absorption at a stellar mass $M_\star \approx 3 \times 10^{10} M_\odot$, which corresponds to $\log v_{MAX} \approx 2.2$ for a reasonable choice of stellar $M = L$. The infall timescale (middle panels) appears also to be correlated with rotation velocity, so that low-mass disks seem to have longer infall timescales. The data suggests that ϵ and τ present similar correlations, a well-known degeneracy (e.g. Ferreras & Silk

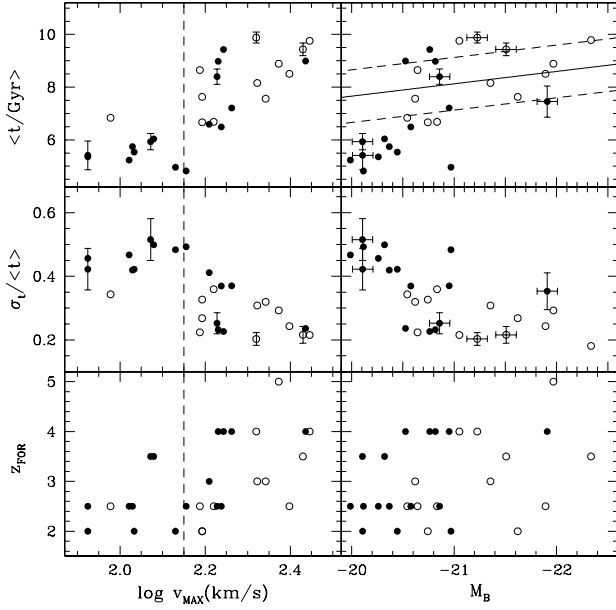


Figure 4. Average (*top*) and RMS (*middle*) values of the best fit stellar age distribution predicted for each galaxy after being evolved to $z = 0$. The vertical dashed line gives the position of the break at $v_{\text{MAX}} = 140 \text{ km s}^{-1}$. Notice that galaxies with larger rotation velocities than this break present a larger scatter towards older ages. The solid line in the top-right panel gives the results from Bell & de Jong (2000) along with a rough estimate of the scatter (dashed lines). The bottom panels show the formation redshift which gives the best fit (see text for details).

2003) which would require more detailed photo-spectroscopic observables to disentangle. Since this analysis is based on broadband photometry which is very much affected by the infamous age-metallicity degeneracy, we decided to test the robustness of our models with respect to a possible systematic effect from the dust correction applied. The appendix compares two possible dust corrections and proves that the bimodality obtained in the star formation efficiency is fairly robust to these corrections.

At this point we should mention the result of Boissier et al. (2001) who claim the efficiency to be uncorrelated with galaxy mass. However, their definition of efficiency is different from ours:

$\epsilon_{\text{g}} = M_{\text{g}} / M_{\text{TOT}}$, where M_{g} is the total gas mass. We can translate between these two definitions of efficiency:

$$\epsilon_{\text{g}} = \frac{M_{\text{g}}}{M_{\text{TOT}}} \quad (4)$$

The total baryon mass in the system is: $M_{\text{TOT}} = M_{\text{g}} + M_{\text{r}} + M_{\text{ej}}$, where the last term refers to the gas mass ejected from stars out of the galaxy. This term can be written as roughly: $M_{\text{ej}} = R M_{\text{r}}$, where R is the outflow fraction defined in x3 and R is the returned fraction, i.e. the fraction of gas ejected from stars (see e.g. Tinsley 1980). If we write the observed gas fraction as $f_{\text{g}} = M_{\text{g}} / (M_{\text{g}} + M_{\text{r}})$, then we can rewrite equation 4 as:

$$\epsilon_{\text{g}} = \frac{1}{f_{\text{g}}} (1 + R) \quad (5)$$

The returned fraction is in the range $0.2 - 0.3$ for most IMFs, so that we can roughly neglect terms $O(R)$ and get the scaling only with respect to the gas fraction. Therefore, our results are compatible with the findings of Boissier et al. (2001) as long as the gas

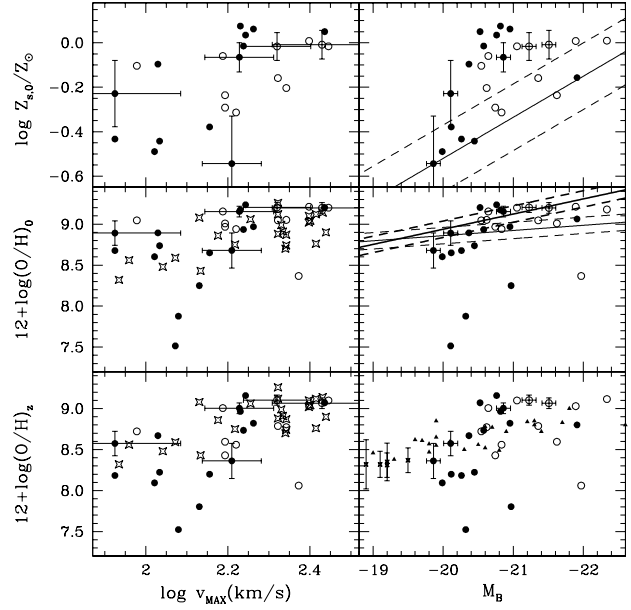


Figure 5. Best average stellar (*top*) and gas phase (*middle, bottom*) metallicities of the sample. The subscript $_0$ refers to metallicities measured after evolving the best-fit SFH to zero redshift, whereas $_z$ refers to a measurement at the observed redshift. The data are shown along with 1- error bars. The solid line in the top-right panel gives the results from Bell & de Jong (2000) along with a rough estimate of the scatter (dashed lines). The stars in the left panels are oxygen gas abundances from a sample of local disk galaxies (Garnett 2002). The stars and triangles in the bottom-right panel give the gas-phase abundance measured in the $z > 0.5$ subsample of moderate redshift galaxies from CADIS (Maier et al. 2004) and DGSS (Kobulnicky et al. 2003), respectively. The lines in the middle-right panel represent the luminosity-metallicity relation from a sample of 53,000 galaxies from SDSS (thick lines; Tremonti et al. 2004) and from the local (K92+NFGS+KISS) sample explored in Kobulnicky et al. (thin lines; 2003 and references therein). A 0.1 dex scatter is assumed.

fraction decreases with galaxy mass. Bell & de Jong (2000) find a correlation between the gas fraction and K band absolute luminosity, namely $f_{\text{g}} = 0.3 + 0.14 (M_K - 20)$, which – assuming a constant ϵ_{g} and using equation 4 – approximately gives a variation in $\log \epsilon_{\text{g}}$ of $+0.5$ dex between bright and faint disks, roughly the same range as the one shown in figure 3 for subsamples in the same redshift range. Brinchmann & Ellis (2000) studied the stellar masses and the star formation rates in a sample of 321 field galaxies out to $z = 1$ and they found a clear decrease of the specific star formation rate – defined as $\epsilon_{\text{g}} = \text{SFR} / M_{\text{r}}$ – with stellar mass (M_{r}). Furthermore, ϵ_{g} was found to increase with redshift. We can write the specific SFR in terms of the efficiency:

$$\frac{\text{SFR}}{M_{\text{r}}} = \frac{f_{\text{g}}^{1.5}}{1 - f_{\text{g}}} \quad (6)$$

The anticorrelation found between ϵ_{g} and stellar mass is thereby a signature of the decreasing gas fraction with galaxy mass. Notice that in figure 3 the subsample with the higher redshift (hollow circles) has a systematically higher star formation efficiency (ϵ_{g}), which is to be expected from equation 6 as the gas fraction will increase with redshift at a fixed rotation velocity.

The bottom panels of figure 3 give the gas outflow fraction, which weakly hints at an anticorrelation with rotation velocity.

Bright disks are redder and faint disks are bluer. This colour trend can be explained either by a range of metallicities — in which the outflow fraction would play the main role — or by a mixed range of ages and metallicities — implying a stronger correlation of ϵ with the luminosity of the galaxy. One can only estimate the weight of these two factors by analyses such as the one presented in this paper. However, the use of a few photometric data points to constrain the star formation history prevents us from extracting an unambiguous conclusion and only allows us to give a semi-quantitative result. The current spectroscopic data from the FDF sample cannot be used for these purposes. Indeed, the spectra from our $z > 0.6$ galaxies only feature one emission line — [OII]/3727Å — with a very low signal-to-noise ratio in the continuum. A detailed spectroscopic analysis on a sample such as this one will doubtlessly give us a clearer prediction of which mechanisms play a key role in the buildup of the stellar component in disk galaxies.

5 AGES AND METALLICITIES

For every choice of star formation history as the one shown in figure 2 one can compute the moments of the age and metallicity distributions. Figure 4 presents the average (top panels) and RMS (middle panels) ages of the stellar component along with a few characteristic 1- σ error bars. The filled and hollow circles correspond to the lower ($0.56 < z < 0.75$) and higher redshift galaxies ($z > 0.75$), respectively. Since the ages and metallicities will be strongly dependent on the redshift of each galaxy, we decided to put all of them at the same redshift. Hence, the values shown in figure 4 correspond to the stellar populations expected *after evolving the predicted star formation histories to $z = 0$* . The bottom panel shows the formation redshift which give the best fit to the observed colours. Higher formation redshifts seem to be favoured by massive disks. The position of the break in the analysis of the star formation efficiency is shown as a vertical dashed line. One sees a clear increase both in the star formation efficiency and the average age as a function of rotation velocity. The massive disks seem to have a slightly smaller RMS scatter in the age, a result obviously generated by their higher star formation efficiency.

Figure 5 presents the results for the average mass-weighted stellar metallicity (*top*) and the gas phase metallicity (*middle*) of the best fit models evolved to zero redshift, and the gas phase metallicity at the observed redshift (*bottom*). Notice that the stellar age and metallicity estimates presented in this paper are in rough agreement with the results from the data presented by Bell & de Jong (2000). Our data does not allow us to pursue an accurate analysis of the ages and metallicities as a function of central surface brightness, but we find a similar correlation as Bell & de Jong with respect to absolute luminosity. The solid line in the top-right panels of figures 4 and 5 show their fits as a function of absolute luminosity. The sample was originally presented as a function of M_K and we used their published $B - K$ colours to show it with respect to M_B . The dashed lines give a rough estimate of the large scatter found in their sample. Gas metallicities are computed assuming a solar abundance ratio in order to translate our metallicities (Z) into O/H measurements. We assume a solar value of $12 + \log(O/H) = 8.7$ (Allende Prieto, Lambert & Asplund 2001). A clear luminosity-metallicity relation can be seen, which is consistent with local observations (K92+NFGS+KISS as referenced in Kobulnicky et al. 2003; thin lines in the middle panel) or with the recent analysis of the oxygen abundances of a large sample ($\sim 53,000$) of galaxies from SDSS (Tremonti et al. 2004; thick lines). The dashed lines represent

a 0.1 dex scatter corresponding to typical error measurements. The triangles in the bottom-right panel are gas metallicity measurements from the Groth Strip survey in the range $0.26 < z < 0.82$ (Kobulnicky et al. 2003) and the star symbols at $M_B > -20$ correspond to moderate redshift galaxies from CADIS (Maier, Meisenheimer & Hippelein 2004). Our results are also compatible with the local estimates of metallicity from the sample of Garnett (2002), shown as star symbols in the bottom-left panel with respect to rotation velocity.

6 DISCUSSION

A simple phenomenological description of the star formation history allows us to explore a large number of possible histories only to be constrained by the observations. In this paper we have used the moderate redshift sample of disk galaxies from the FORS Deep Field. Comparing the aperture photometry in several passbands between data and simple models of chemical enrichment across a wide spectral range (UV- K) we have found an increase of the star formation efficiency — as defined in equation 1 — with rotation velocity. A clear threshold appears around $v_{MAX} \sim 140 \text{ km s}^{-1}$ so that slowly rotating disks present uniformly low star formation efficiencies and younger stellar populations with a larger spread of stellar ages. More massive disks show a wide range of efficiencies. A similar conclusion was reached by Ferreras & Silk (2001) on the analysis of the local sample of UMa cluster disks from Verheijen (2001). The thorough analysis of observational data across a wide spectral range — from the radio to the UV — probing the stellar and gas component of a sample of 928 nearby disk galaxies led Gavazzi, Pierini & Boselli (1996) to conclude that, to first order, mass is the driving parameter of galaxy evolution. They suggested that a positive correlation between star formation efficiency and galaxy mass should be invoked to explain the observations. Furthermore, this trend is consistent with the analysis of Dalcanton et al. (2004) who also find a threshold in v_{MAX} when exploring the thickness of dust lanes in disks. They relate this threshold to a tradeoff between the two main causes of turbulence in the ISM, namely supernova feedback and gravitational instabilities. The former is the dominant factor in low-mass disks and produces a higher velocity dispersion in the gas, which results in lower star formation efficiencies. In contrast, Dalcanton et al. suggest turbulence in massive disks to be mainly caused by gravitational instabilities. The lower velocity dispersion implied by these instabilities results in an increased efficiency of star formation. Along similar lines, Silk (2001) suggested a Schmidt-like star formation law:

$$\dot{\sigma} \propto \frac{\rho_g}{v_{SN}} ; \quad (7)$$

where $\dot{\sigma}$ is the disk angular velocity, ρ_g is the cold gas velocity dispersion and v_{SN} is a characteristic velocity defined from supernova feedback as the specific momentum injected by supernovae per unit star formation rate. In this framework, the results from figure 3 suggest a major change in the ratio $(\dot{\sigma}/v_{SN})$ at around $v_{MAX} \sim 140 \text{ km s}^{-1}$.

This bimodal trend has been explored in a large dataset of 120,000 galaxies drawn from the SDSS (Kauffmann et al. 2003). Low-mass galaxies were found to have younger stellar populations and low concentrations, with some of these systems having experienced recent star formation. At stellar masses above $3 \times 10^{10} M_\odot$, galaxies feature older populations and the high concentrations typical of spheroidal systems. In the light of our

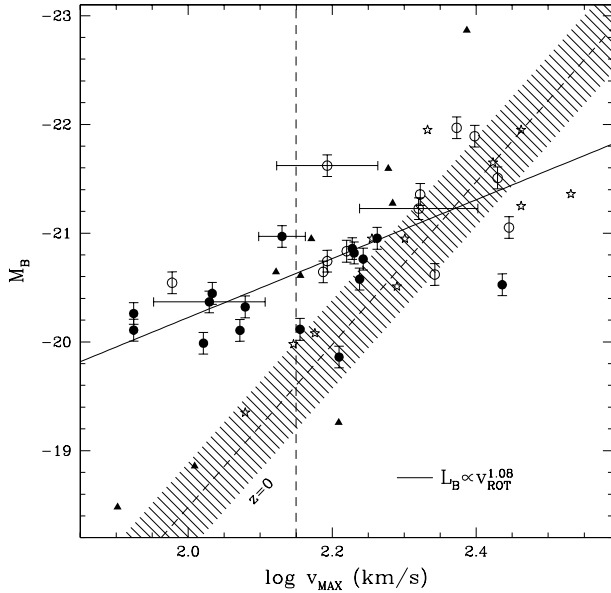


Figure 6. The Tully-Fisher relation at moderate redshift. The filled and hollow circles correspond to the $z < 0.75$ and $z > 0.75$ FDF subsamples, respectively. A few characteristic error bars in $\log v_{\text{MAX}}$ are shown. The stars and triangles represent the ($z > 0.4$) data from Vogt et al. (1997) and the field disks from Milvang-Jensen et al. (2003), respectively. The solid line is a linear fit to the FDF data. The fit to the local sample of Pierce & Tully (1992) is also shown as a dashed line, with a shaded region representing the scatter.

models, this spheroidal-like behaviour of large disks reveals the high star formation efficiency as expected in bulges or elliptical galaxies. Furthermore, a recent paper (Kannappan 2004) has explored the gas-to-star mass ratios using $u - K$ colour as a proxy. The sample of 35,000 galaxies was extracted from the SDSS and 2MASS databases and a similar bimodal trend was found, with a threshold around a similar stellar mass, i.e. $2 - 3 \times 10^{10} M_{\odot}$. Our results confirm this bimodal trend in disk galaxies out to $z = 1$.

The star formation histories proposed in this paper for disk galaxies allow us to determine reliable evolution corrections and rest-frame luminosities. Figure 6 shows the Tully-Fisher relation with respect to rest-frame M_B . The model absolute luminosities are very similar to those already presented by Ziegler et al. (2002) and Böhm et al. (2004) for which the k corrections were obtained using the population synthesis models of Möller et al. (2001). As a comparison, we also show (at $z > 0.4$) the field sample of Milvang-Jensen et al. (2003; triangles) as well as the sample from the DEEP Groth Strip Survey (Vogt et al. 1997; stars). The solid line is a fit to our data, whereas the local Tully-Fisher relation is shown as a dashed line and the scatter is represented by the shaded region (Pierce & Tully 1992). The FDF sample clearly gives a shallower Tully-Fisher relation with respect to the local sample. The small size and scatter in the sample of Milvang-Jensen et al. (2003) prevents us from making any estimate of their mismatch with respect to the local TFR. Vogt et al. (1997) give a result which is more compatible with the observations at $z = 0$. However, their selection favours large disks which biases the sample towards early-type systems. Böhm et al. (2004) suggested this slope change could be caused by a mass-dependent luminosity evolution. In this paper we

do not attempt to relate the bright and slowly rotating disks from the FDF sample with local low-mass disk galaxies. In fact, a naïve one-to-one mapping of local and high redshift Tully-Fisher relations would result in an anticorrelation between star formation efficiency and galaxy mass. We only use the aperture photometry of the FDF disk galaxies in order to constrain their star formation histories. The rotation velocities are then used to assign a “size” parameter to each galaxy. The evolution of the slowly rotating disks from our analysis to $z = 0$ results in a population of bright disks which are not seen in local surveys. Hence, our results conclude that these objects do not have local counterparts, in agreement with Lilly et al. (1998) who find a population of small and bright disks at $z > 0.7$ which do not have counterparts in the local galaxy census. A simple estimate of the contribution from young stars can be done if we consider the combination of two simple stellar populations, an old one which represents the underlying population and a young one with a fractional mass contribution f_Y which corresponds to the recent episode of star formation. We can then relate the actual luminosity of the galaxy (L) to the luminosity of the underlying old stellar component (L_O), namely

$$\frac{L}{L_O} = \frac{M}{M_O} \frac{1}{f_Y} = 1 + \frac{f_Y}{1 - f_Y} \frac{L_Y}{L_O}; \quad (8)$$

where $M = M_O + M_Y$ is the mass-to-light ratio, and the subscripts O and Y denote the old and young component, respectively. Let us consider a small fractional contribution, say $f_Y = 0.1$. Assuming a metallicity $\log(Z/Z_{\odot}) = 0.5$ for both components, and an age of 6 Gyr for the old population – corresponding to a formation redshift $z_F = 5$ for a galaxy at $z = 0.75$ – this 10% contribution in mass from young stars translates into $M_B = M_B - M_{B,Y} = 2.5 \log(L_{B,Y}/L_B) = 1.9$ mag for a young component with $t_Y = 0.1$ Gyr and -0.95 mag for $t_Y = 0.5$ Myr. A couple of Gyr after the episode has subsided (i.e. $t_O = 8$ Gyr and $t_Y = 2$ Gyr) the same 10% contribution implies $M_B = -0.36$ mag. Hence, small episodes of star formation could account for the presence of these bright and slowly rotating disks. We should mention that no strong evolution is expected in v_{MAX} from mass accretion from $z = 1$ to the present time. In our adopted Λ CDM cosmology accretion is mostly suppressed at low redshift by the growth factor in linear theory. Indeed, the disk galaxy models of van den Bosch (2002) show that the rotation curves do not change more than 5% in this redshift range.

Nevertheless, this does not invalidate the correlation between v_{MAX} and the star formation efficiency, but rather, strengthens it. The progenitors of the local slowly rotating disks without any recent star formation will be below the detection threshold of the FDF sample, which implies even lower efficiencies should be considered at low v_{MAX} , in agreement with the analysis of Ferreras & Silk (2001). Their prediction of a steepening of the slope of the TFR with redshift implies disks with $v_{\text{MAX}} < 100 \text{ km s}^{-1}$ at $z = 1$ should be fainter than $M_B = -18$, a result which is also consistent with the models of Boissier & Prantzos (2001). It is intriguing that there is evidence for very modest episodes of late star formation even in nearby early-type galaxies (Trager et al. 2000). Theory strongly suggests that such episodes should increase with redshift. This is commonly accepted as plausible in galaxy compact groups and protoclusters, where the merger frequency is high. However a comparably strong statement in the environs of typical disk galaxies is puzzling. Very few dwarfs are found near the Milky Way or M31 relative to the predictions of the commonly accepted CDM model. The usual explanation is that companion dwarfs have been stripped of gas and indeed of stars, as suggested by the evidence for tidal

streams (Ferguson et al. 2002) and the ongoing disruption of the Sagittarius dwarf galaxy (e.g. Majewski et al. 2003). Such episodes must have been more frequent in the past if theory – which predicts an order of magnitude more dwarfs than are observed – is to be reconciled with the observations. Dwarf disruption will include both compression of gas in the dwarf core as well as gas ejection into the gas reservoir of the host galaxy. Both effects will result in transient episodes of star formation. These enhanced phases of star formation, although individually modest and short-lived, could account for as much as half of the current stellar mass. Such minibursts are also inferred to have occurred in the Milky Way from the past history of star formation inferred from analysis of chromospheric age indicators in the local stellar population (Rocha-Pinto et al. 2000). The inferred stages of episodic brightening at a lookback time of 5 Gyr or more could help account for the brightening that we infer of small disks in the past. We conclude that more data are badly needed at moderate redshift in the M_B 18 range if we are to develop a full understanding of the Tully-Fisher relation.

APPENDIX A: THE EFFECT OF DUST CORRECTIONS ON THE MODEL PREDICTIONS

Dust correction introduces colour variations which can have an important effect in the model predictions. In this paper we have used the dust corrections presented in Böhm et al. (2004) which follow Tully & Fouqué (1985), so that the correction depends on the inclination. However, a systematic effect could arise if this dust correction were dependent on v_{MAX} as presented in Tully et al. (1998). These authors find that luminous disks could suffer more reddening than low-mass disks, thereby introducing a systematic trend towards older populations in massive disks. In this appendix we present the results for a single grid of star formation histories choosing a formation redshift $z_F = 5$ and two extinction corrections: the one used in this paper – only dependent on inclination – and the one from Tully et al. (1998) – where both the inclination and rotation velocity determine the reddening. For the latter we also assume no extinction in face-on galaxies. Figure A1 shows the model predictions for the star formation efficiency (*top*), infall timescale (*middle*) and average stellar ages (*bottom*) as a function of v_{MAX} . The left panels show the change of these parameters with respect to the uncertainty, and the right panels give the parameters themselves for these two extinction laws. One can see that the parameters vary mostly within the 1 uncertainties, preserving the strong bimodal trend in star formation efficiency. No significant systematic trends were seen either by Böhm et al. (2004) when comparing these two dust correction prescriptions. Hence, within the model uncertainties already discussed in the paper, we conclude that the trend seen with respect to star formation efficiency or age is unaffected by different dust correction prescriptions.

ACKNOWLEDGMENTS

This research has been supported in part by PPARC Theoretical Cosmology Rolling Grant PPA/G/O/2001/00016 (IF), by the Volkswagen Foundation (I/76520), and by the “Deutsches Zentrum für Luft- und Raumfahrt” (50 OR 0301). We acknowledge receipt of a JREI grant from PPARC to provide the computing facilities. We would like to thank Frank Van den Bosch for useful discussions. The anonymous referee is gratefully acknowledged for a very constructive criticism of this paper.

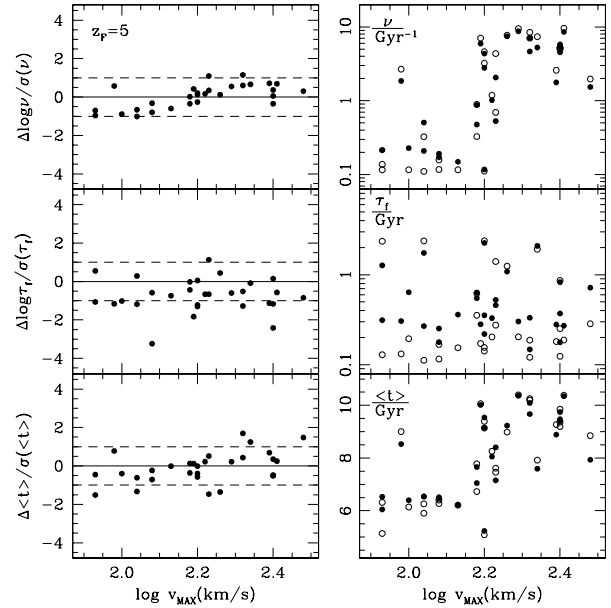


Figure A1. Effect of a different dust correction in the model predictions for the star formation efficiency (*top*), infall timescale (*middle*) and average stellar age (*bottom*) as a function of v_{MAX} . A single formation redshift was chosen ($z_F = 5$) with two different extinction corrections. The left panels show the variation in the model predictions with respect to the 1 uncertainty. The right panels give separately the model predictions for these two corrections, namely: Tully & Fouqué (1985; solid dots) and Tully et al. (1998; hollow dots).

REFERENCES

- Allende Prieto, C., Lambert, D. L. & Asplund, M., 2001, *ApJ*, 556, L63
- Arimoto, N. & Yoshii, Y., 1987, *A&A*, 173, 23
- Appenzeller, I., et al. 2000, *Messenger*, 100, 44
- Bell, E. F. & de Jong, R. S., 2000, *MNRAS*, 312, 497
- Bertin, E. & Arnouts, S., 1996, *A&AS*, 117, 393
- Böhm, A., et al. 2004, *A&A*, 420, 97
- Boissier, S. & Prantzos, N., 1999, *MNRAS*, 307, 857
- Boissier, S., Boselli, A., Prantzos, N. & Gavazzi, G., 2001, *MNRAS*, 321, 733
- Boissier, S. & Prantzos, N., 2001, *MNRAS*, 325, 321
- Brinchmann, J. & Ellis, R. S., *ApJ*, 536, L77
- Bruzual, A. G. & Charlot, S., 2003, *MNRAS*, 344, 1000
- Chabrier, G. 2003, *PASP*, 115, 763
- Dalcanton, J. J., Yoachim, P. & Bernstein, R. A. 2004, *ApJ*, 608, 189
- Ferguson, A. M. N., Irwin, M. J., Ibata, R. A., Lewis, G. F. & Tanvir, N. R., 2002, *AJ*, 124, 1452
- Ferreras, I., & Silk, J., 2001, *ApJ*, 557, 165
- Ferreras, I., & Silk, J., 2003, *MNRAS*, 344, 455
- Garnett, D. R., 2002, *ApJ*, 581, 1019
- Gavazzi, G., Pierini, D. & Boselli, A., 1996, *A&A*, 312, 397
- Giallongo, E., Menci, N., Poli, F., D’Odorico, S. & Fontana, A., 2000, *ApJ*, 530, L73
- Heidt et al. 2003, *A&A*, 398, 49
- Kannappan, S. J., 2004, *ApJ*, 611, L89
- Kauffmann, G., et al., 2003, *MNRAS*, 341, 54
- Kennicutt, R. C., 1998a, *ARA&A*, 36, 189

- Kennicutt, R. C., 1998b, *ApJ*, 498, 541
 Kobulnicky, H. A., et al. 2003, *ApJ*, 599, 1006
 Larson, R. B., 1974, *MNRAS*, 169, 229
 Lilly, S., et al. 1998, *ApJ*, 500, 75
 Maier, C., Meisenheimer, K. & Hippelein, H., 2004, *A&A*, 418, 475
 Majewski, S., Law, D. R., Johnston, K. V., Skrutskie, M. F. & Weinberg, M. D., 2003, *astro-ph/0311522*
 Möller, C. S., Fritze-v.Alvensleben, U., Fricke, K. J. & Calzetti, D., 2001, *Ap&SS*, 276, 799
 Pierce, M. J. & Tully, R. B., 1992, *ApJ*, 387, 47
 Rocha-Pinto, H. J., Scalo, J., Maciel, W. J. & Flynn, C., 2000, *ApJ*, 531, L115
 Salpeter, E. E., 1955, *ApJ*, 121, 161
 Schmidt, M. 1959, *ApJ*, 129, 243
 Silk, J., 2001, *MNRAS*, 324, 313
 Spergel, D. N., et al. 2003, *ApJS*, 148, 175
 Thielemann, K. F., Nomoto, K. & Hashimoto, M. 1996, *ApJ*, 460, 408
 Trager, S. C., Faber, S. M., Worthey, G. & González, J. J., 2000, *AJ*, 119, 1645
 Tremonti, C. A., et al. 2004, *ApJ*, in press, *astro-ph/0405537*
 Tully, R. B. & Fouqué, P. 1985, *ApJS*, 58, 67
 Tully, R. B., Pierce, M. J., Huang, J.-S., Saunders, W., Verheijen, M. A. W. & Witchalls, P. L. 1998, *AJ*, 115, 2264
 van den Hoek, L. B. & Groenewegen, M. A. T. 1997, *A&AS*, 123, 305
 van den Bosch, F. C., 2002, *MNRAS*, 332, 456
 Verheijen, M. A. W., 2001, *ApJ*, 563, 694
 Vogt, N. P. et al. 1997, *ApJ*, 479, L121
 Vogt, N. P. et al. 2000, in *Dynamics of galaxies: from the Early Universe to the Present*, F. Combes, G. A. Mamon & V. Charmandaris, eds. ASP. Conf. Ser. 197, 435
 Ziegler, B. L., Böhm, A., et al., 2002, *ApJ*, 564, L69
 Ziegler, B. L., Böhm, A., Jäger, K., Heidt, J. & Möllenhoff, C., 2003, *ApJ*, 598, L87

This paper has been typeset from a \TeX / \LaTeX file prepared by the author.